PROCEEDINGS
Volume 2-Gas

ERDA
Symposium on Enhanced Oil & Gas Recovery

Albright

Camelot Inn, Tulsa, Oklahoma

September 9-10, 1976

ENERGY RESEARCH AND DEVELOPMENT ADMINISTRATION

DIVISION OF OIL, GAS, AND SHALE TECHNOLOGY

IN COOPERATION WITH

UNIVERSITY OF TULSA • OIL & GAS JOURNAL

The University of Tulsa

OIL&GAS JOURNAL

SEISMIC MAPPING OF HYDRAULIC FRACTURES MADE IN BASEMENT ROCKS

by

J. N. Albright
R. J. Hanold

Los Alamos Scientific Laboratory
Los Alamos, NM 87545

ABSTRACT

A study of the phase arrival times and polarization of microseismic signals has provided sufficient information to define the size and orientation of hydraulic fractures created at a depth of 3 km in dry hot basement rocks. Seismic signals in the 750 to 2250 Hz bandpass have been detected by geophones positioned in a borehole adjacent to the well from which the fracture originates. Preliminary mapping of the fracture shows it to be vertical, or nearly so, at least 140 m in length and 300 m in height, and striking NNW.

INTRODUCTION

For the last three years, the Los Alamos Scientific Laboratory has been actively investigating the potential for, and problems associated with, extracting geothermal energy in those parts of the United States that contain dry, hot rock at moderate depths. At sufficient depth, rock hot enough to be potentially useful as an energy source exists everywhere, and in many places it is at depths shallow enough to be reached at moderate cost with existing equipment. In the Los Alamos concept, a man-made geothermal reservoir would be formed by drilling into an identified region of suitabley hot rock, and then creating within the rock a very large surface area for heat transfer by use of large-scale hydraulic-fracturing techniques developed by the oil industry. After a circulation loop is formed by drilling a second hole into the top of the fractured region, the heat contained in this reservoir would be brought to the surface by the buoyant circulation of water. The water in the loop would be kept liquid by pressurization at the surface, thereby increasing the rate of heat transport up the withdrawal hole compared to that possible with steam. Figure 1 is a schematic diagram of a man-made geothermal system.

LASL'S GEOTHERMAL ENERGY PROJECT

The initial geothermal source demonstration presently being conducted by LASL is located on the Jemez Plateau in that part of the Rocky Mountains extending into northern New Mexico. As a result of relatively recent volcanic

Illustrations at end of paper.

activity, a large amount of heat is still retained in the rock underlying the area within a few kilometers of the surface. On the basis of extensive studies and field experiments, the "Fenton Hill" site (about 32 km west of Los Alamos) was selected for development of the first dry hot rock energy experiment. The primary objective of the dry hot rock geothermal energy extraction experiment is to investigate and demonstrate the techniques of drilling into hot granitic rock, fracturing it by hydraulic pressure, producing connected circulation loops and then circulating water to extract the heat and transport it to the surface.

The first exploratory borehole drilled at the Fenton Hill site was designated Geothermal Test Hole No. 2 (GT-2). The Precambrian granitic surface was reached at 733 m and drilling continued to a final depth of 2932 m. Numerous experiments were conducted in various zones extending from 2789 m to the bottom of the borehole. A series of hydraulic-fracture-initiation, fracture-extension, and pumping experiments were conducted in these zones to determine principal tectonic stress, stress variations, and the leak-off rate of the fracturing fluid. A fracture near the bottom of GT-2 was eventually extended to a radius of approximately 70 m and measurements were performed to characterize this fracture. The first energy extraction borehole (EE-1) was drilled adjacent to GT-2 to a depth of 3064 m with a measured bottom-hole temperature of 205°C. The first downhole circulation loop was attempted by employing directional drilling techniques to turn the EE-1 borehole to intercept the fracture created in GT-2. It was important to obtain the dimensions and orientation of the hydraulic fracture to achieve intersection of the fracture system with the second borehole (EE-1). Development of downhole instrumentation capable of characterizing the hydraulic fracture system in the high-temperature and high-pressure borehole environment was therefore required.

ACOUSTIC FRACTURE MAPPING TECHNIQUES

A downhole triaxial geophone package was employed to detect acoustic signals from discrete fracturing events as the hydraulic fracture was extended. Records obtained with this instrumentation established the existence of detectable microseismic events uniquely associated with the reinflation and extension of a hydrualic fracture previously created in GT-2. Signals from the microseismic events contained sufficient information to determine the foci of the events. By assuming that the locus of the events originated from the fracture plane intersecting GT-2, the fracture can be mapped in space (size, shape, and orientation) and time (growth during injection). The borehole and fracture geometry and the geophone positions for the experiment are shown in Fig. 2. The hydraulic fracture to be mapped originated at 2.8 km in a lined section of GT-2 that had been perforated and then milled out. Four observation stations were occupied in succession in an uncased section of EE-1 by a three-component geophone package capable of being repeatedly repositioned and coupled directly to the borehole walls. The magnetic orientation of the package at each depth was determined from an Eastman Whipstock magnetic survey tool attached to the bottom of the geophone package.

Fluid injection into the hydraulic fracture lasted for a period of 1 hour. Each geophone station was occupied in turn for 15 min, and at the termination of the experiment the first station was reoccupied for another 15 min. During the time the geophone package was positioned at the first location, the fracture was being inflated. Fracture extension commenced at some time during the occupation of the last three stations. The fracture maps obtained are horizontal projections of microseismic event foci occurring within an inclination of ± 10 degrees of the horizontal at the specific depth of measurement. In effect then, the maps represent projections of horizontal bands across the fracture face in which seismic activity is occurring. The observed signals, which are bandpass filtered between 750 to 2250 Hz, exhibit both compressional wave, and shear wave arrivals. Hence from a determination of the arrival times of each phase the distance to the focus of an event can be measured. Furthermore, since the signals were recorded by orthogonally oriented geophones, hodograms or Lissajous figures of particle velocity can be used to determine the azimuthal approach of the signal.

ANALYSIS OF DISCRETE MICROSEISMIC SIGNALS

The events, originally recorded as analog signals on magnetic tape, were digitized at 50 μs/sample and bandpass filtered between 750 and 2250 Hz for analysis. This filter selection was empirically determined as a compromise in avoiding high noise levels at low frequencies and aliasing in spectral analyses. The signals exhibit discernible p- and s-wave arrivals. The time interval between the arrivals can be measured, and the propagation velocity of the respective waves is known: therefore, the distance to the source of events can be determined. Generally, an s-wave arrival can be identified with little difficulty. It shows up clearly within the p-wave coda of signals as a high-amplitude arrival on vertical geophone records and as a phase and amplitude change on the horizontal geophone records. This is not the case with the p-wave onset, because the signal is emergent above the ambient noise level. The combined error in estimating the time interval between the p- and s-wave arrival times is about ± 0.5 ms, resulting in a 4-m uncertainty in distance determinations.

Provided that the time interval between p- and s-wave arrivals from an event can be determined and that the wave velocities are known, only the arrival direction of the signal is needed to define the focus of an event. Because p-waves are linearly polarized in the direction of signal propagation, the azimuth and inclination of the signal polarization describes the direction to an event focus. The signal azimuth and inclination can be determined by inspecting velocity hodograms of two components of the velocity amplitude of a signal constructed from the geophone recordings. Figure 3 is a sequence of hodograms of a signal arrival recorded by the horizontal geophones. Clearly shown is the noise before p-wave arrival, p-wave onset, linear polarization of the p-wave defining the signal azimuth, and s-wave onset. The inclination to the source can be determined from a similar hodogram, one axis of which would necessarily be the vertical component of velocity amplitude.

MEASUREMENTS OF CONTINUOUS RADIATION

Continuous seismic radiation was also observed during these experiments. The signal is clearly seen when records containing the microseismic events are low-pass filtered at 30 Hz. Although a thorough study of these signals has not been made, the radiation appears useful in determining fracture orientation. The dominant frequency of the radiation is 7 Hz, which corresponds to the frequency of pump strokes during injection. The signal appears only after the volume of fluid injected into the fracture approaches that necessary for extension.

A hodogram of the horizontal velocity amplitude components of the radiation, Fig. 4, shows that the radiation is elliptically polarized with the azimuth of the major axis of the ellipse closely corresponding to the fracture direction that is defined in maps of microseismic event foci. As a consequence, inferences can be made that the radiation is excited by pumping induced pressure fluctuations in the wellbore from which the fracture originates, and that the signal detected results from disturbances traveling along the fracture faces.

Measurements based on records of continuous radiation are of limited use, because without substantial advances in theory neither the distance to a hydraulic fracture from an observation station nor the size of a fracture can be determined. Nonetheless, the method has provided additional measurements of fracture orientation, and for this reason, is important to develop.

FRACTURE MAPPING EXPERIMENTS

Figure 5 shows a projection to the horizontal at a depth of 2.81 km of the foci of events occurring during the initial 13.5 m^3 (3560 gal) inflation of the GT-2 fracture. EE-1 is located at the origin; radii are given for the distance to foci in terms of the time interval between p- and s-wave arrival times in milliseconds, and also in terms of the estimated distance to the events. Activity was clustered and is probably occurring near the GT-2 borehole. The trace of the fracture plane strikes NNW. Magnetic north at this depth in EE-1 is indicated on Fig. 5.

When the station at 2.81 km was reoccupied, fluid injection had been stopped at 45 m^3 and the system had been shut in at the operating pressure. The events that occurred during this interval are shown in Fig. 6. Even though injection had ceased, activity was pronounced. Comparison with Fig. 5 shows that in the period between successive observations at this depth, activity had increased to extend along a line exceeding 140 metres. The orientation of the fracture is clearly defined as N27W. Figure 7 combines the data of Figs. 5 and 6 and shows how the locus of events along the fracture has grown with time. These data suggest that the fracture should be able to be defined from geophones positioned in the borehole in which the fracture originated.

Hydraulic fracture microseismic event foci were also determined at depths of 2.94 km and 3 km during inflation and extension of the fracture. The data were of sufficient quality and number to define the fracture orientation and length. The activity was observed to be less pronounced than at the 2.81 km depth and it occurred over a shorter band. The strike of the fracture exhibited a considerable counterclockwise rotation of 30°. The length of the fracture at 3 km is considerably less than that at 2.8 km. This observation, combined with the reduced activity at 3 km is evidence that the fracture probably terminates near this depth. Pronounced activity and the greatest fracture length is found at 2.8 km - an indication that the fracture extends upward from this depth. Induced potential logs indicate that the fracture probably extends upward at least to 2.7 km. The total vertical dimension of the fracture must therefore exceed 300 m.

The apparent warp of the fracture is best shown by the three-dimensional perspectives given in Figs. 8 and 9. The horizontal lines denote equivalent depths. In the model the fracture is shown as symmetric about the GT-2 wellbore, and the shape of the fracture is represented as a regular form with lateral dimensions corresponding to those determined from microseismic event foci. The orientation of the fracture with respect to magnetic north changes 30° counterclockwise in the depth interval in which the measurements were made. This amount of rotation is beyond the range of the experimental error. One interpretation of the apparent rotation is that the hydraulic fracture itself may not be warped, but rather the direction of the ambient magnetic field may change over the vertical distance of measurement. Because conventional magnetic borehole surveys of GT-2 before fracturing did not show any anomaly at the depths in question, this is probably not the case. If, on the other hand, the warp of the fracture is real, it must be produced by the stress distribution changing with depth in the host rock.

CONCLUSIONS

When taken collectively the results of each of these measures of fracture size and orientation gives confidence that the immediate goal of drilling through a hydraulic fracture targeted in space by remote geophone sensors may soon be realized. The downhole acoustic experiment has proven to be a successful field technique. One area of major concern in the true orientation of the seismic sonde downhole. It is important to determine the position of the triaxial geophone cradle once the instrument package is locked into the borehole wall.

ACKNOWLEDGMENT

The introductory text contains excerpts from Los Alamos Scientific Laboratory Reports authored by members of the Geothermal Energy Group.

REFERENCES

1. Smith, M. C., "Geothermal Energy," Los Alamos Scientific Laboratory report LA-5289-MS (May 1973).

2. West, F. G., "Regional Geology and Geophysics of the Jemez Mountains," Los Alamos Scientific Laboratory report LA-5362-MS (August 1973).

3. Pettitt, R. A., "Testing, Drilling, and Logging of Geothermal Test Hole GT-2, Phase III," Los Alamos Scientific Laboratory report LA-5965-PR (June 1975).

4. Dennis, B. R., et al, "Development of High-Temperature Acoustic Insturmentation for Characterization of Hydraulic Fractures in Dry Hot Rock," 22nd International Instrumentation Symposium (May 1976).

5. Blair, A. G., Tester, J. W., and Mortensen, J. J., Comps., "LASL Hot-Dry-Rock Geothermal Project Annual Report, July 1, 1975-June 30, 1976," Los Alamos Scientific Laboratory Report (to be published).

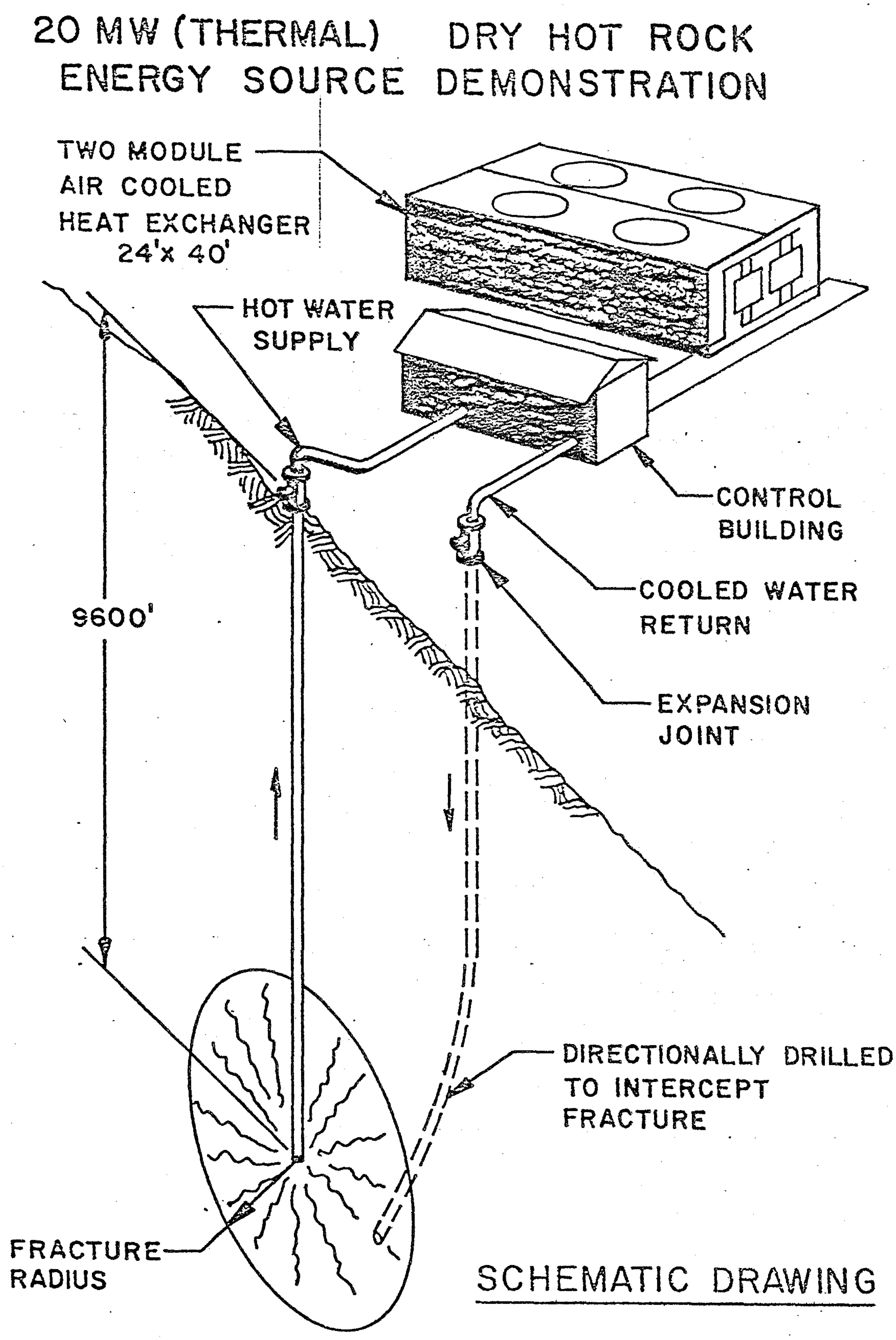

Figure 1. Dry-Hot-Rock Geothermal-Energy System Developed by Hydraulic Fracturing.

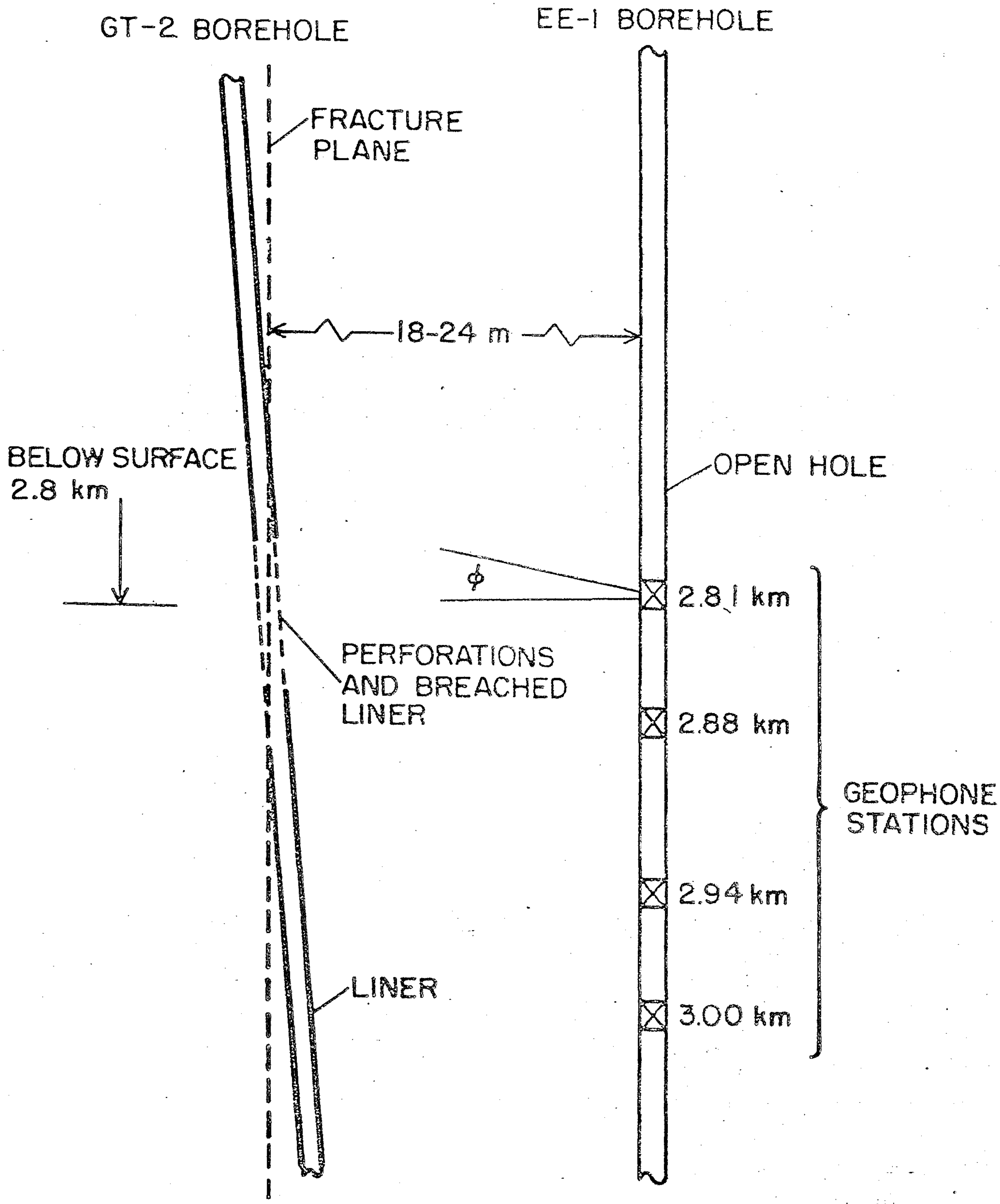

Figure 2. Downhole Acoustic Fracture Mapping Experiment.

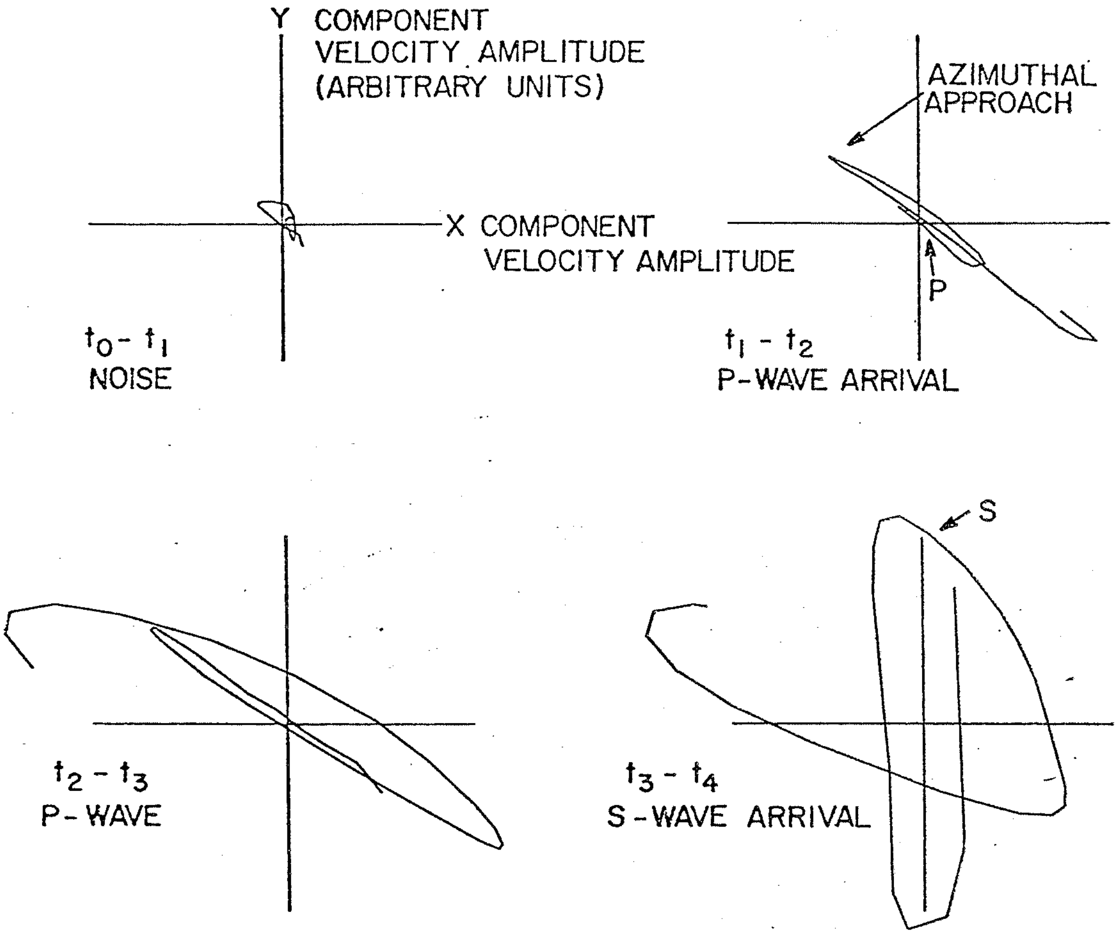

Figure 3. Representative Hodograms of a Microseismic Signal (8-ms total time) Received at the Horizontal Geophone.

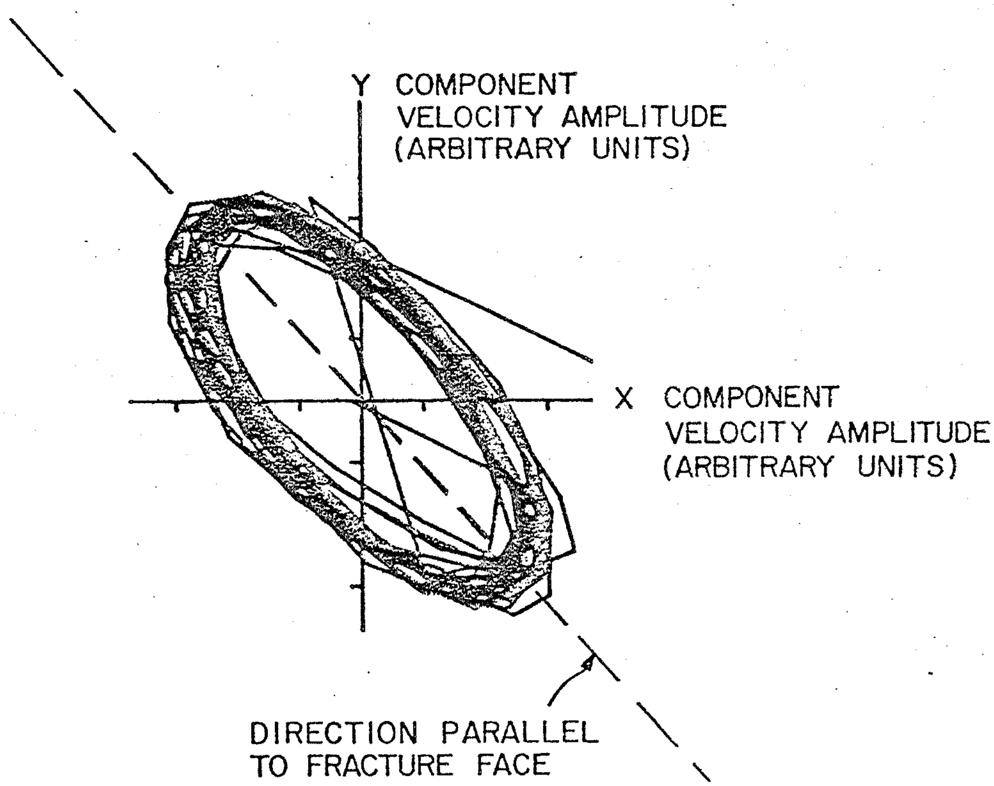

Figure 4. A Hodogram Representative of the Continuous Seismic Radiation from the GT-2 Fracture Induced by Pumping.

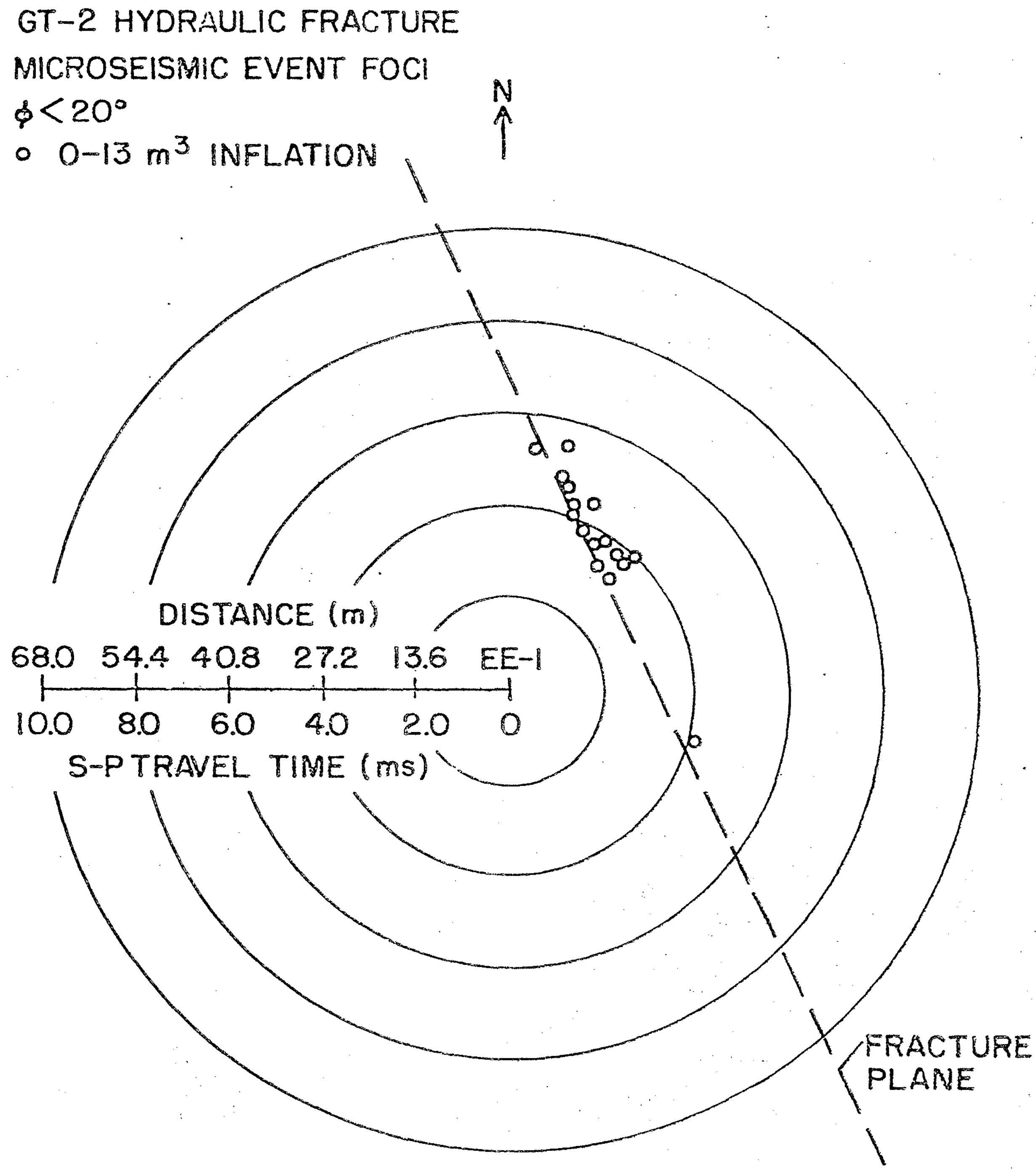

Figure 5. Foci of Microseismic Events Recorded at a Depth of 2.81 km During the Initial Period of Inflation.

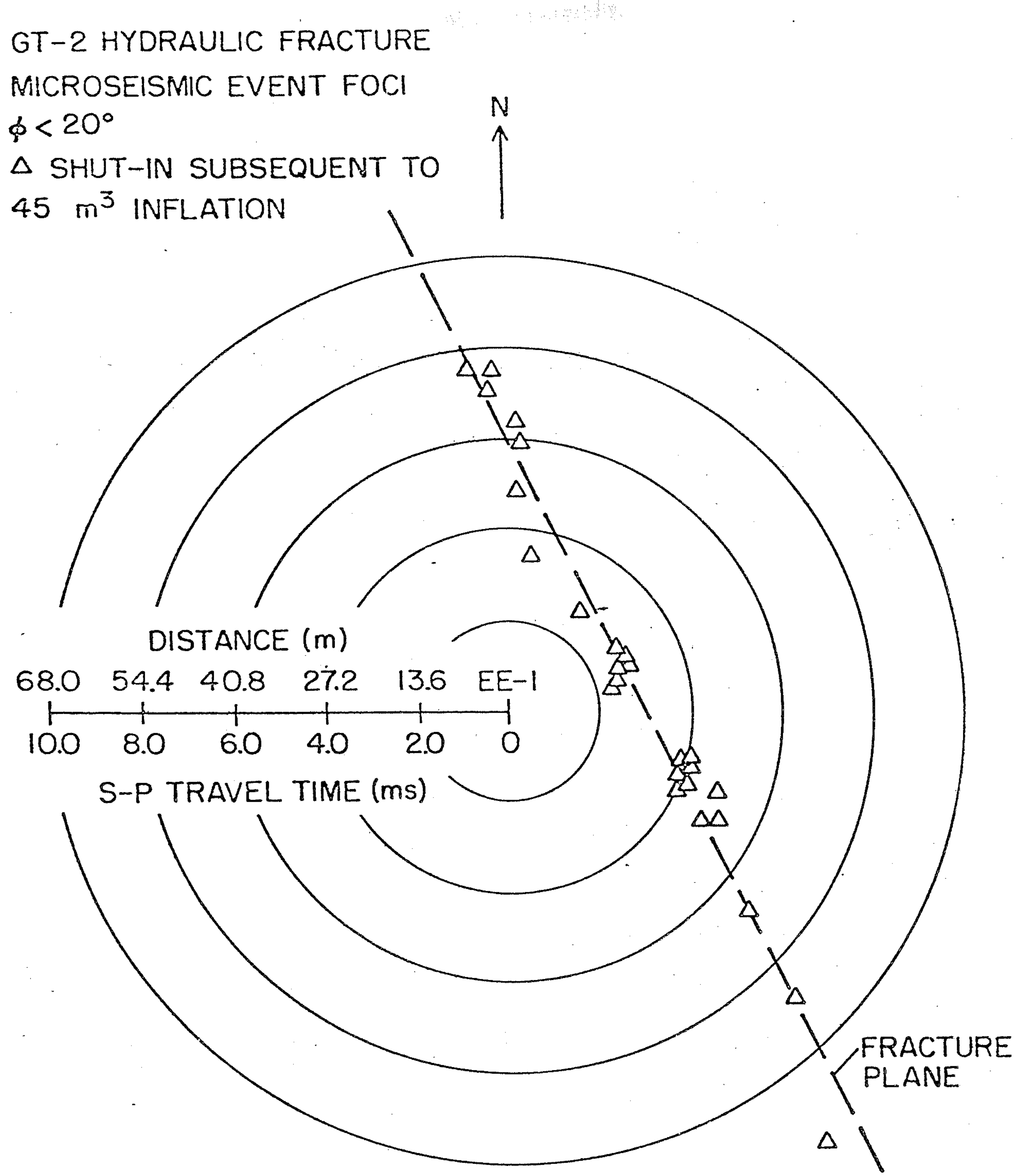

Figure 6. Foci of Microseismic Events Recorded at a Depth of 2.81 km During Shut-In Subsequent to Inflation.

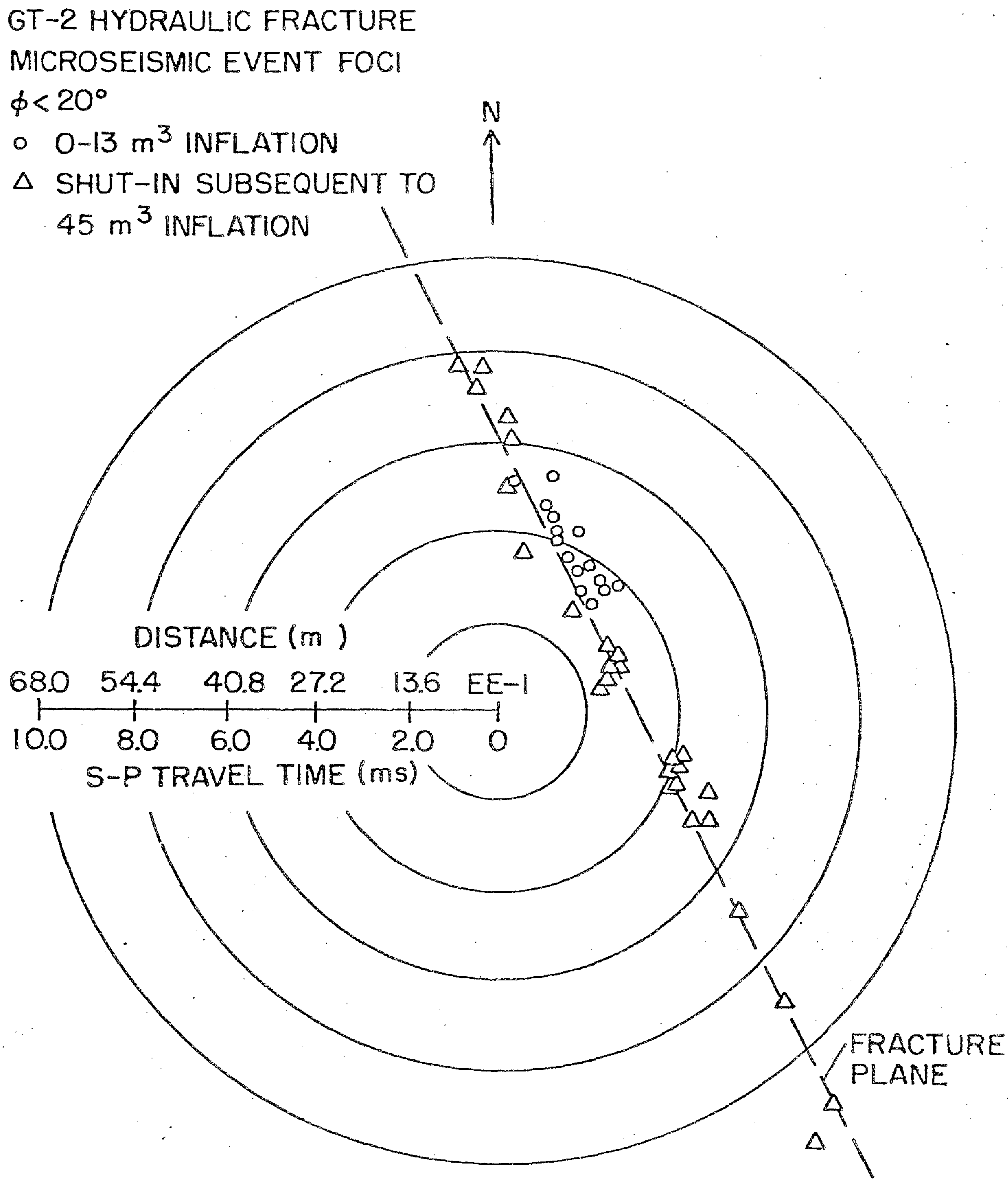

Figure 7. Foci of Microseismic Events Recorded at a Depth of 2.81 km (Combined Data of Figure 5 and 6).

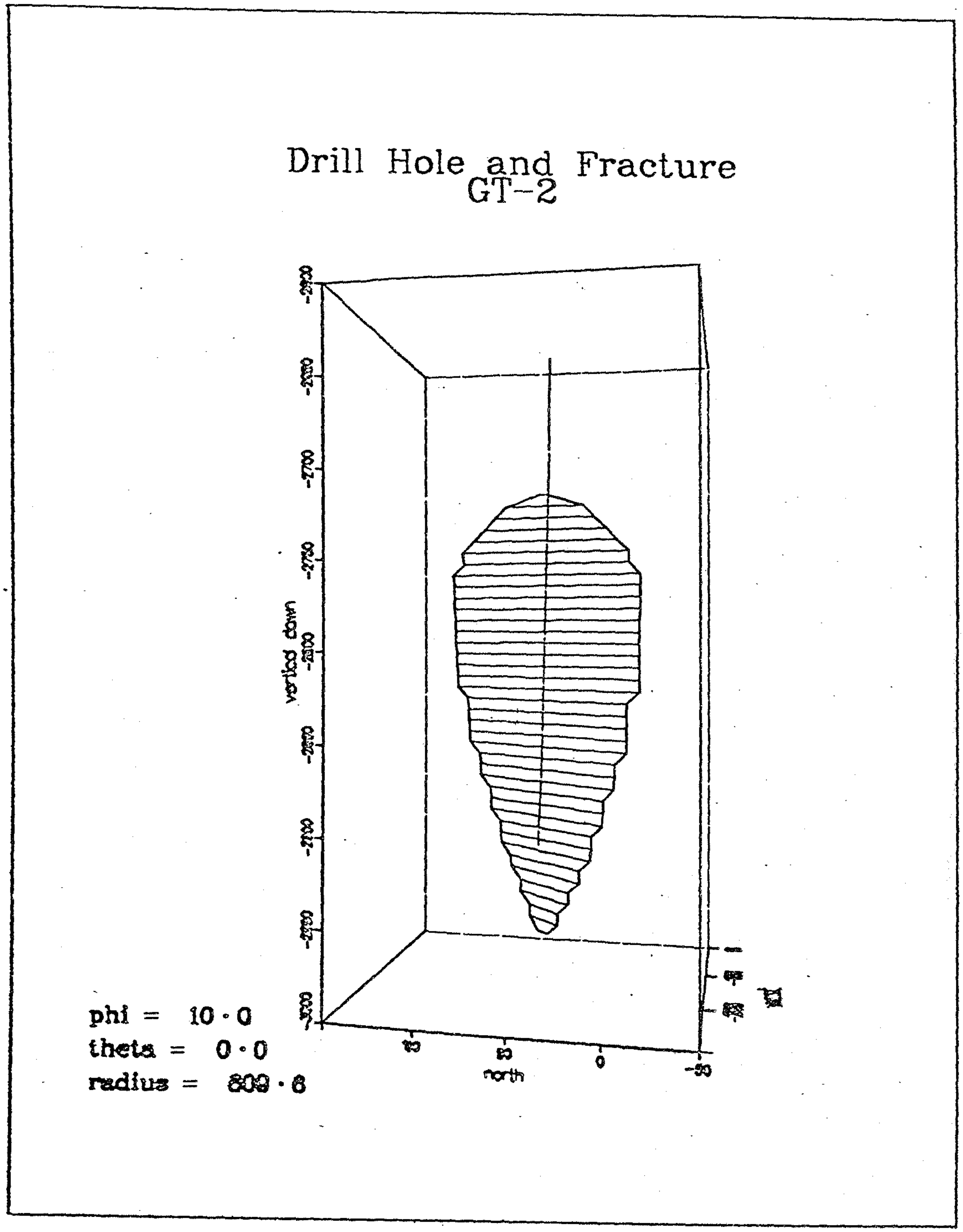

Figure 8. Three-Dimensional Perspective of the Fracture Originating in GT-2 (at 10° to the Fracture Surface at 2.81 km).

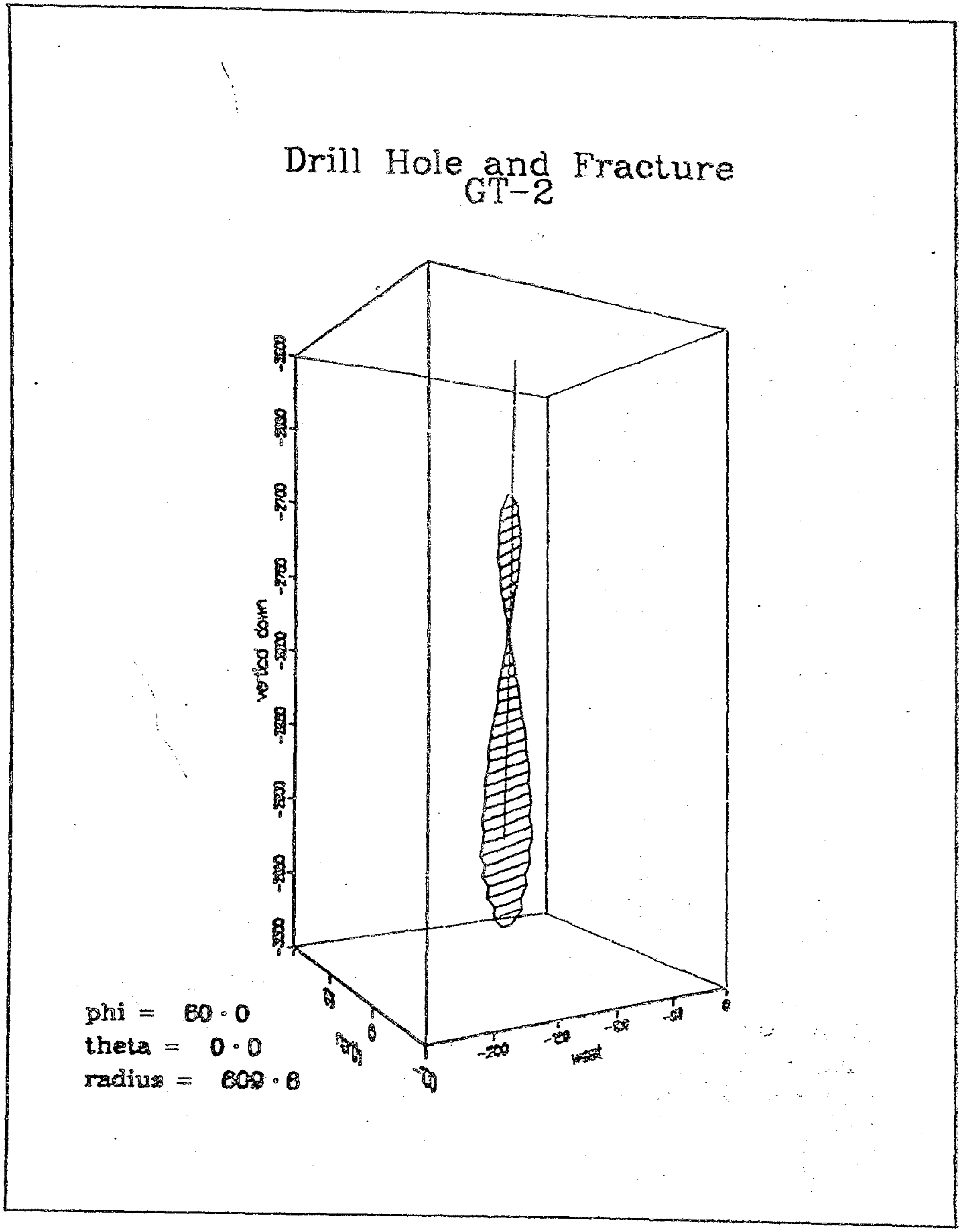

Figure 9. Three-Dimensional Perspective of the Fracture Originating in GT-2 (at 60° to the Fracture Surface at 2.81 km).